Indian Journal of Pure & Applied Physics
Vol. 57, October 2019, pp. 743-749

Influence of oxide film surface morphology and thickness on the properties of gas sensitive nanostructure sensor

G Behzadi Pour* & L Fekri Aval

Department of Physics, East Tehran Branch, Islamic Azad University, Tehran, Iran

Received 20 January 2018; accepted 29 April 2019

In this study, the gas sensitive metal-oxide semiconductor (MOS) nanostructure sensors based on Ni thin film have been fabricated. The influences of SiO_2 film surface morphology and thickness on the response (R%) and electrical properties of the sensors have been investigated at 150 °C. The surface morphology of the SiO_2 film has been characterized by scanning electron microscopy (SEM) and atomic force microscopy (AFM). The C-V curves of the MOS nanostructure sensors in pure nitrogen and 2 % hydrogen have been reported as well. For the SiO_2 film thicknesses of 14, 65 and 74 nm the measured flat-band voltages (V_{FB}) are 0.7, 1.5 and 2 V, respectively. The responses of different sensors in 2% hydrogen for SiO_2 film thicknesses of 14 and 74 nm are 84% and 32%, respectively. The MOS nanostructure sensors exhibited good response to the hydrogen gas, with excellent sensitivity. The MOS nanostructure sensor based on Ni thin film and SiO_2 film thickness of 14 nm shows high response and sensitivity.

Keywords: Nanostructure, Morphology, Sensitive, Thin film

1 Introduction

Hydrogen with flammable range (4-75%) is a gas that cannot be detectable by human sense[1]. Hydrogen sensors by absorb hydrogen molecules produce an electrical signal. There is a continued need for hydrogen gas sensor in power generation, chemical, automotive and stationary applications[2]. They are compact and more suitable for portable applications. Also measurement of hydrogen concentration is required for production of ammonia and methanol[3]. Performance of the hydrogen sensors is investigated based on the electrical, electrochemical, mechanical, optical and acoustic changes. The hydrogen sensors based on the electrical properties are classified in to work function, resistance, current/voltage and electrical conductivity change[4]. The performance of the MOS nanostructure sensors is based on the work function change. The metal gate of the MOS structure is catalytic layer that can absorb the hydrogen molecules. In gas sensitive MOS nanostructure sensors, hydrogen atoms diffuse through the catalytic metal gate and at the interface of metal gate and oxide film giving rise to a dipole layer[5-8]. We have recently reported the hydrogen sensors using Pd nanoparticles capacitor sensor at the room temperature[9-12]. The sensing mechanism of the MOS nanostructure sensors is based on the shift in the C–V curve. The thicknesses of the oxide film, gas concentration and temperature are three important parameters on the response of the MOS hydrogen sensor[13].

Palladium (Pd), nickel (Ni) and platinum (Pt) due to catalytic surface are used as a metal gate in many of hydrogen gas sensors. The Ni as the metal gate is used in the MOS nanostructure separately or mostly in form Pd/Ni nanocomposite. Sun *et al.*[14] reported the effects of Ni contents on the performance of the Pd/Ni-based hydrogen sensor. They synthesized the Pd/Ni alloy nanocrystals (with a Ni content ranging from 0 to 60%) and was suggested an optimal Ni content of 16% to fabricate hydrogen sensors with fast response and best sensitivity in a wide gas pressure range. In other study, for hydrogen detection the Pd/Ni alloy have been electrodeposited on carbon fibers[15]. That paper was reported two types of Pd/Ni alloy nanostructures (nanofilm and nanoparticles) and showed the hydrogen sensing depends on the synthesis of volume expansion of the particles or film, the change of energy barrier at the interface and formation of the Pd–H. The Pd, Ni and Pt are used combination with nanowires, nanoparticles, carbon nanotubes and graphene[16-27]. Phan *et al.*[28] described the reliability of hydrogen sensor based on bimetallic Ni-Pd/graphene composites. They showed a small enhancement of sensitivity, fast recovery, and minimum hysteresis effect at the optimal Ni/Pd percentage (Ni/Pd ~7%) and also was reported the

*Corresponding author (E-mail: ghobadbehzadi@yahoo.com)

addition of Ni to PdNPs results in a reduction of the hysteresis effect and reliability on the hydrogen sensor. Moreover, Bhati *et al.*[29] introduced the Ni/ZnO nanostructures for detection of low hydrogen concentration (1ppm) at temperature of 75 °C. They reported the hydrogen sensing behavior structural and morphological Ni/ZnO thin film strongly depends on doping concentration. The thickness and quality of the oxide film as an insulator in MOS nanostructure sensor determine the capacitance and the V_{FB} of the sensor. In this research, the influence of oxide film surface morphology and thickness on the properties and sensitivity of the MOS nanostructure sensor is investigated. The fabrication and characterization of three types of the Ni/SiO_2/Si sensors have been reported. The response, electrical properties and sensing mechanism of the MOS nanostructure sensor to hydrogen concentration were studied at 150 °C.

2 Material and Methods

In this study the hydrogen gas sensitive MOS nanostructure sensors based on Ni thin film have been fabricated. The schematic of the MOS nanostructure sensor was illustrated in the Fig. 1 (a). Dry oxidation was done in thermal chemical vapor deposition furnace. For three samples dry oxidation was done separately at 5, 25 and 30 min. On the SiO_2 film a 100 nm film of Ni and on the backside of the semiconductor a 100 nm film of Au has been deposited. The ohmic contact to the backside of semiconductor was made by evaporating. The wires were connected to the Ni thin film and Au film. For C-V measurement of the MOS nanostructure sensor the wires were attached to the LCR meter. The set up includes LCR meter modules (GPS-3135B) that can be interfaced to a PC. When the MOS nanostructure sensor is biased by negative voltage, the accumulation region gives way to depletion region. As it can be seen in Fig. 1 (b) the capacitor of depletion region is series with the capacitor of the accumulation region. In Fig. 1 (b), t_{ox} is the thickness of the oxide film and X_d is the width of depletion layer. By increase of negative voltage to the MOS nanostructure sensor, the semiconductor enters an inversion region.

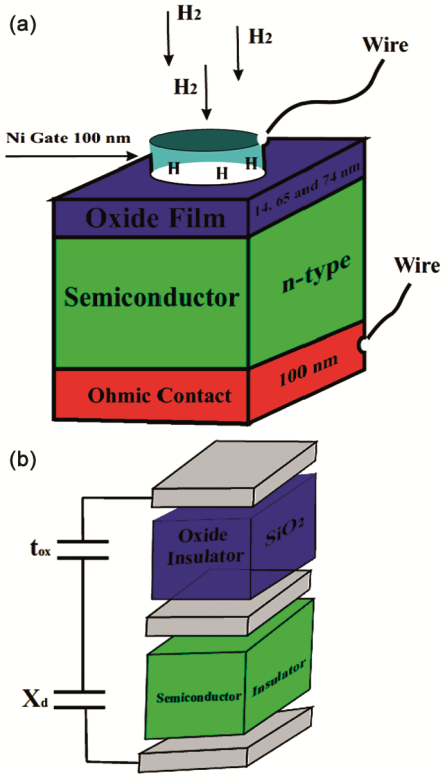

Fig.1 — (a) Schematic of the MOS nanostructure sensor and (b) capacitance of depletion region (ε_s) is series with the capacitance of the accumulation region (ε_{ox}).

3 Results and Discussion

For three hydrogen MOS nanostructure dry oxidation was done separately at 5, 25 and 30 min. For oxidation times 5 min, 25 min and 30 min the oxide thicknesses were 14 nm, 65 nm and 74 nm. The surface morphologies of the SiO_2 films were characterized by DME software AFM module (DS 95-50-E scanner). Figure 2 shows the AFM images of the SiO_2 film in different oxidation times. For a better comparison the image profile of summits in a certain direction for SiO_2 films have been plotted in Fig. 2. The expression of summits is used to measure peak height above the brain profile. The average roughness was characterized by DME software and for the oxidation times 5 min, 25 min and 30 min were 11 nm, 2.9 nm and 2.8 nm, respectively. The SEM images of the SiO_2 film in different oxidation times were presented in Fig. 3. The C-V curves of the MOS nanostructure sensors in pure N_2 and at 150 ˚C have been shown in Fig. 4. As it can be seen in Fig. 4, the electrical capacitance of the MOS nanostructure sensors in the accumulation region is constant. The V_{FB} is a boundary between the accumulation region and depletion region. The V_{FB} is given by[30]:

$$V_{FB} = \frac{W_{MS}}{q} - \frac{Q_t\, t_{ox}}{\varepsilon_{ox}\varepsilon_0 A} \quad \ldots (1)$$

Where W_{MS} is the difference between Ni and Si work function and Q_t is the trapped charges in the SiO_2 film. For an ideal MOS sensor the V_{FB} is zero.

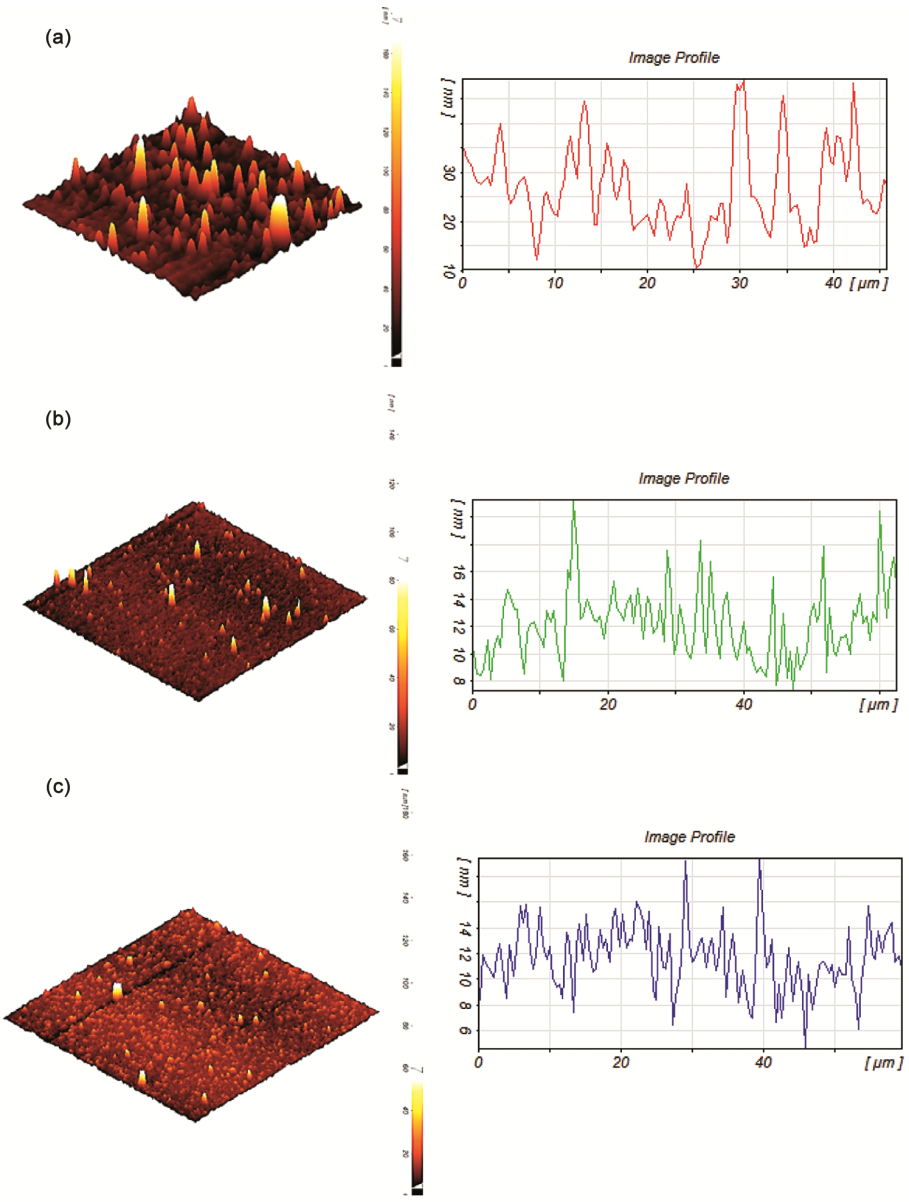

Fig. 2 — The AFM image and the image profile of summits in a certain direction for oxide with oxidation time (a) 5 min, (b) 25 min and (c) 30 min.

Figure 5 shows the energy diagram of a real MOS structure in unbiased condition. For real MOS structure due to the work function difference between metal and semiconductor the $W_{MS} \neq 0$. The importance of energy barriers between metal-SiO_2 and SiO_2-Si is prevention of free flow from metal gate to semiconductor. Therefore, for a real MOS sensor the V_{FB} is not zero. For Ni thin film the work function is 5.2 eV and for silicon the work function varies from 4.7 eV. For the MOS structure, a typical value of V_{FB} shift is 0.5 V. The measured V_{FB} for SiO_2 thicknesses of 14, 65 and 74 nm were 0.7, 1.5 and 2 V, respectively. This difference is related to the trapped charges in the SiO_2 film. Figure 6 shows the C-V curves of the MOS capacitor sensors in 2% hydrogen concentration at 150 °C. The depletion region of C-V curves falls at negative voltage, which indicated that the V_{FB} is decreased. The shift of the V_{FB} is due to absorbed atoms of hydrogen at the interface of metal gate and SiO_2 film and give rise to a dipole layer. This dipole layer cusses a change in the work function of the Ni thin film[31,32]. The response (R %) of the MOS nanostructure sensors to hydrogen can be obtained from:

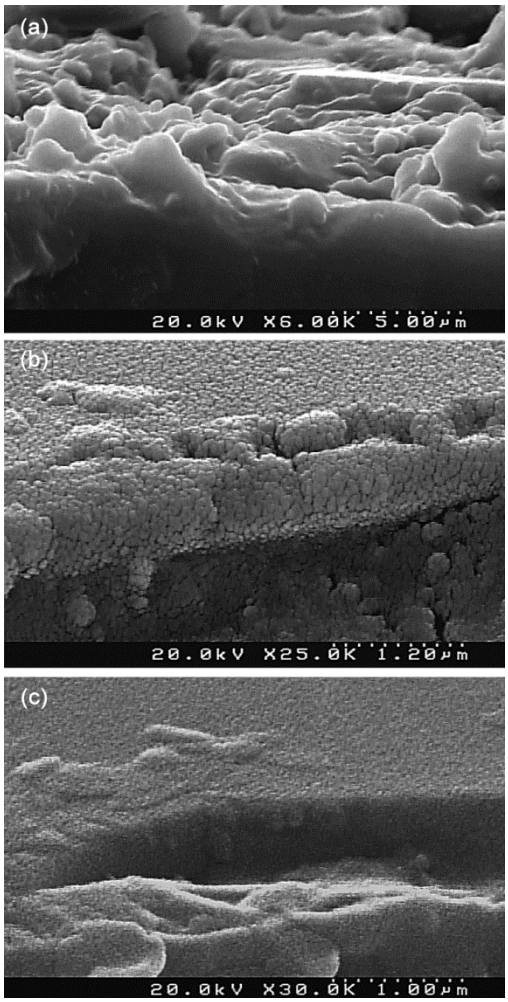

Fig. 3 — The SEM images of the SiO_2 film in different oxidation times (a) 5 min, (b) 25 min and (c) 30 min.

$$R\ (\%) = \left(\frac{C_H}{C_N} - 1\right) \times 100 \qquad \ldots (2)$$

Where C_H is the capacitance in 2% hydrogen and C_N is the capacitance in pure nitrogen. The response of three MOS nanostructure sensors was illustrated in Fig. 7. The response for SiO_2 thicknesses of 14, 65 and 74 nm were 84%, 44% and 32%, respectively. The literature[13] shows the response of a MOS sensor was decreased from 90% to 40% by increase the SiO_2 thicknesses from 2.4 nm and 14.8 nm. The sensitivity mechanism of this study is the association of trap

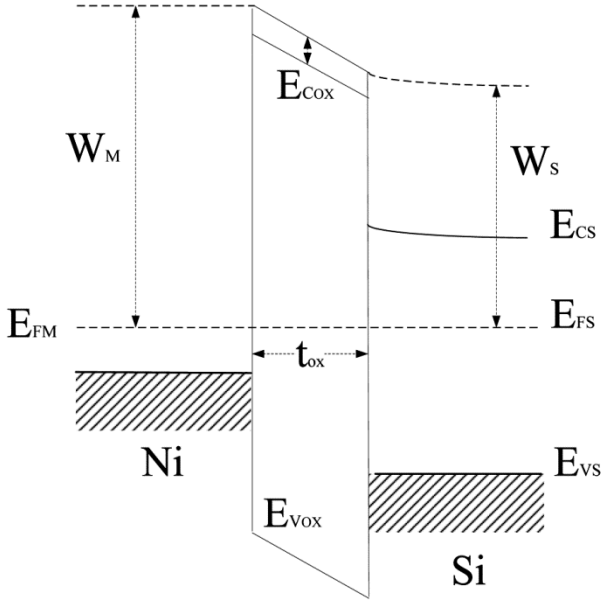

Fig. 5 — The energy diagram of a real MOS structure in unbiased condition.

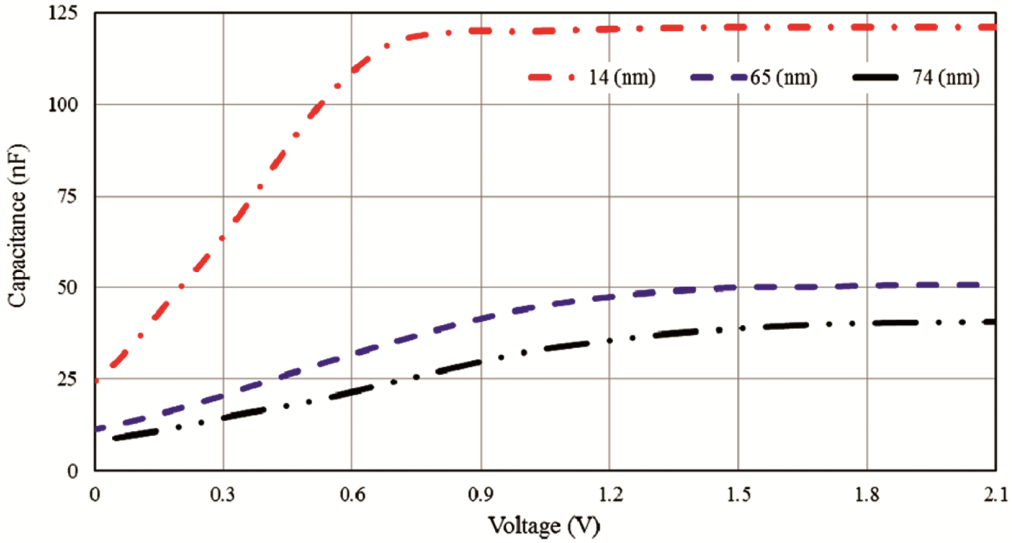

Fig. 4 — The C-V curves of the MOS nanostructure sensors in pure N_2 and at 150 ˚C.

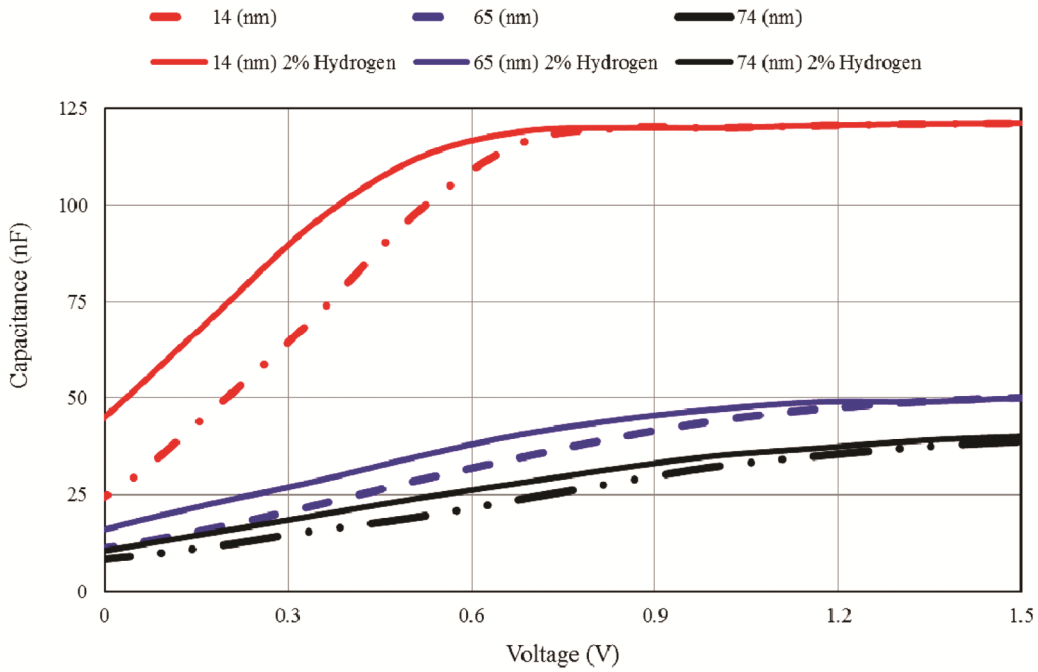

Fig. 6 — The C-V curves of the MOS nanostructure sensors in 2% hydrogen concentration at 150 ˚C.

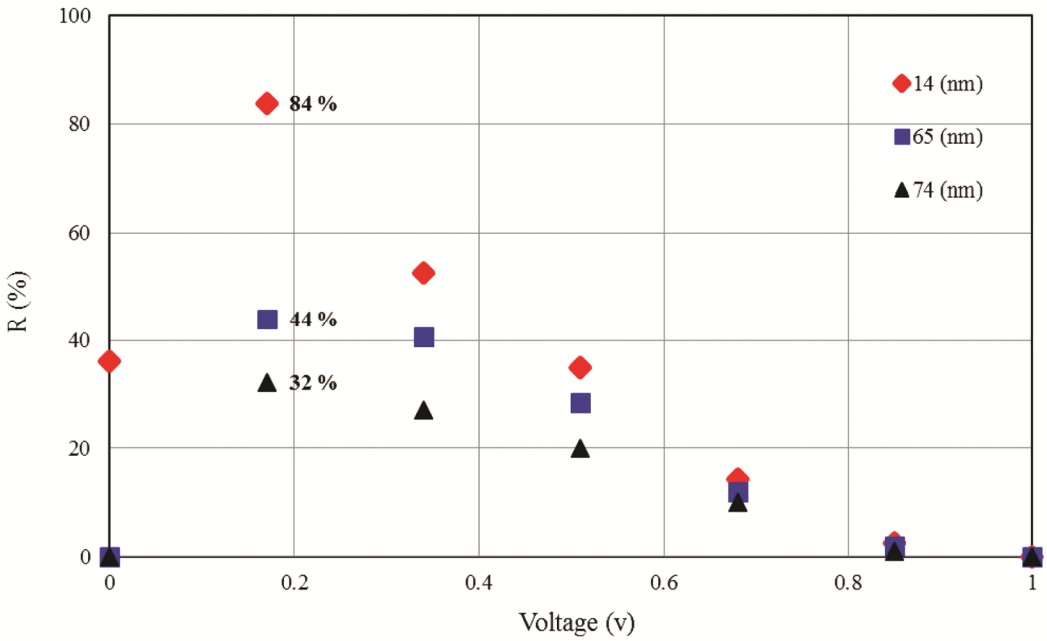

Fig. 7 — The response of three MOS nanostructure sensors.

states in the Si-SiO_2 interface. The association of trap states in the interface is much greater for thinner SiO_2 film and cusses a stronger dipole layer in the interface. This mechanism was shown in Fig. 8**.** The trap states and the thicknesses of the SiO_2 films were shown by bubbles and dash lines respectively.

Figure 8 shows by increasing the SiO_2 film thickness the density of trap states have been decreased. Comparison of different hydrogen gas sensors was shown in Table 1. As can be seen in Table 1, the hydrogen sensors based on the Pd/SnO_2 electrode showed the high response at both room and high

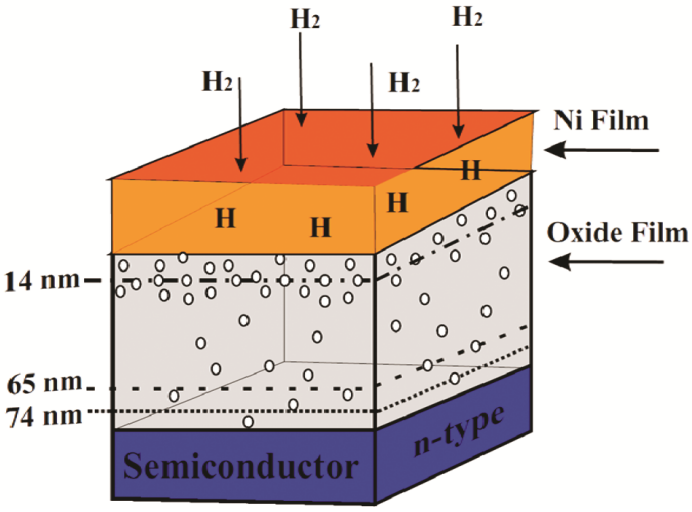

Fig. 8 — The sensing mechanism of the association of trap states in the Si-SiO_2 interface.

Table 1 — Comparison of different hydrogen gas sensors.

Electrode	Temperature Range (°C)	Detection limit (%)	Typical sensor	Response (%)	Reference
Ni thin film	150	2	MOS	84	This work
Pd/SnO_2	200	0.005-0.05	Resistance	80	(Ref. 33)
Pd/SnO_2 nanocrystalline	RT 125	0.1	Current	95 120	(Ref. 34)
Pd/WO_3/SiC	200	1	Current	89	(Ref. 35)
Pd/TiO_2 nanocube	150	0.6-1	Resistance	40.8	(Ref. 36)
Pd/TiO_2/Polypyrrole	RT	1	Resistance	8.1	(Ref. 37)
Pd/Ag	80-180	0.01-0.5	Resistance	14.26	(Ref. 38)
Pd-Ag/graphene	70-170	0.01-0.5	Resistance	16.2	(Ref. 39)
Pd/MoS_2	RT	0.005-1	Resistance	35.3	(Ref. 40)
Pd/titania nanotubes	RT	0.05-1.6	Resistance	88	(Ref. 41)

temperature[33,34]. Liu *et al.*[35] investigated the hydrogen sensor using the Pd-WO_3-SiC Schottky diode. They found upon exposure to 10,000 ppm H_2/air, the diodes show a maximum hydrogen response of 89%. In other study, fast response of hydrogen sensor using Pd nanocube-TiO_2 nanofiber composites reported in literature[36]. That paper showed the response of the hydrogen sensor is 40.8% at working temperature of 150 °C. Moreover, Zou *et al.*[37] prepared the hydrogen gas sensor based on the Pd/TiO2@PPy nanocomposite. They indicated the high selectivity, excellent reproducibility and good stability of the Pd–TiO_2@PPy nanocomposite make it suitable for hydrogen detection. As can be seen in table 1, the hydrogen sensors using the Pd/Ag electrode showed the response 14% up to 16% at temperature range of 70 °C to 180 °C[38,39]. Also, the hydrogen sensor prepared by Pd/MnS_2 has been investigated in earlier study[40]. That paper revealed that the response of the Pd/MoS_2 hydrogen sensor was 35.3% when exposed to 1% hydrogen concentration, while the pristine MoS_2 showed no reaction. Wu *et al.*[41] described the hydrogen sensor using Pd nano-rings supported by titania nanotubes substrate at room temperature. They showed when the water content was 17.5 wt%, the sensor revealed a sensitivity of 88% at 1.6% hydrogen concentration. Comparison of different hydrogen sensors showed the MOS nanostructure sensor based on the Ni thin film revealed a high response at temperature of 150 °C.

4 Conclusions

In this study the influence of SiO_2 film surface morphology and thickness on the properties of gas sensitive MOS nanostructure sensor have been investigated. The response (R%) and sensing

mechanism of the three MOS nanostructure sensors in different voltages have been measured. The C-V curves of MOS nanostructure sensors in pure nitrogen and different applied voltages show that the V_{FB} was increased from 0.7 V to 2 V. The C-V curves of the MOS nanostructure sensors in 2% hydrogen concentration show that the depletion region falls at negative voltage, which indicated that the V_{FB} is decreased. The shift in the V_{FB} is due to absorbed atoms of hydrogen at the interface of metal gate and SiO_2 film and gives rise to a dipole layer. This dipole layer cusses a change in the work function of the Ni thin film. The response for SiO_2 thicknesses of 14, 65 and 74 nm were 84%, 44% and 32%, respectively. The sensitivity mechanism of this study is that of the association of trap states in the Si-SiO_2 interface. The association of trap states in the interface is much greater for thinner SiO_2 film and cusses a stronger dipole layer in the interface.

Acknowledgement

This research work was supported by the department of physics, East Tehran Branch, Islamic Azad University.

References

1 Carcassi M N & Fineschi F, Energy, 30 (2005)1439.
2 Boon B L, Bousek J, Black G, Moretto P, Castello P, Hubert T & Banach U, *Int J Hydrogen Energy*, 35 (2010) 373.
3 Czuppon T A & Knez S A & Newsome D S, *Hydrogen, Kirk-Othmer Encyclopedia of Chemical Technology*, *(*Wiley: New York), (1996) 884.
4 Hubert T, Boon B L, Black G & Banach U, *Sens Actuators B*, 157 (2011) 329.
5 Eunyeong L, Junmin L, Jinseo N, Wonkyung K, Taeyoon L, Sunglyul M & Wooyoung L, *Int J Hydrogen Energy*, 37 (2012) 14702.
6 Linke S, Dallmer M, Werner R, Moritz W, *Int J Hydrogen Energy*, 37 (2012) 17523.
7 Preeti P, Srivastava J, Mishra V & Dwivedi R, *Solid State Sci*, 11 (2009) 1370.
8 Chi L, Zhi C & Kozo S, *Sens Actuators B*, 122 (2007) 556.
9 Leila F A & Mohamad E, *Electron Mater Lett*, 13 (2017) 77.
10 Ghobad B P & Leila F A, *Results Phys*, 7 (2017) 1993.
11 Ghobad B P & Leila F A, *NANO*, 12 (2017) 1750096.
12 Ghobad B P & Leila F A, *Micro Nano Lett*, 13 (2017) 149.
13 Chi L & Zhi C, *Int J Hydrogen Energy*, 35 (2010) 12561.
14 Ling S, Minrui C, Xing P, Bo X & Min H, *Int J Hydrogen Energy*, 41 (2016) 1341.
15 Ou Y J, Si W W, Yu G, Tang L L, Zhang J & Dong Q Z, *J Alloys Compd*, 569 (2013) 130.
16 Jixiang D, Minghong Y, Xun Y & Hong L, *Opt Fiber Technol*, 19 (2013) 26.
17 Ohodnicki P R, Baltrus J P & Brown T D, *Sens Actuators B*, 214 (2015) 159.
18 Isaac N A, Ngene P, Westerwaal J, Gaury J, Dam B, Schmidt A O & Bikos G, *Sens Actuators B*, 221 (2015) 290.
19 Jin H Y, Bum J K & Jung S K, *Mater Chem Phys*, 133 (2012) 987.
20 Amit S, Ashwani K, Samta C, Yogendra KG & Ramesh C, *Sens Actuators B*, 213 (2015) 252.
21 Yogendra K G, Ravish J, Sunil K T, Agrawal R D & Ramesh C, *Sens Actuators B*, 176 (2013) 453.
22 Palmisano V, Filippia M, Baldi A, Slaman M, Schreuders H & Dam B, *Int J Hydrogen Energy*, 35 (2010) 12574.
23 Jixiang D, Minghong Y, Xun Y, Kun C & Junsheng L, *Sens Actuators B*, 174 (2012) 253.
24 Eunsongyi L, Jun M L, Eunyoung L, Jin S N, Jin H J, Bumsuk J & Wooyoung L, *Thin Solid Films*, 519 (2010) 880.
25 Abdelhamid B, Chao Z, Polona U, Carla B, Rony S, Marie G O & Marc D, *Int J Hydrogen Energy*, 38 (2013) 2565.
26 Minghong Y, Yan S, Dongesheng Z & Desheng J, *Sens Actuators B*, 143 (2010) 750.
27 Zilli D, Bonelli P R & Cukierman A L, *Sens Actuators B*, 157 (2011) 169.
28 Duy T P & Gwiy S C, *Int J Hydrogen Energy*, 39 (2014) 20294.
29 Vijendra S B, Sapana R, Mattia F, Matjaz V & Mahesh K, *Sens Actuators B*, 225 (2018) 588.
30 Bentarzi H, Transport in Metal-Oxide- Semiconductor Structure; Mobile Ions Effects on the Oxide Properties, (Springer: New York), (2011) 39.
31 Sze S M, *Physics of Semiconductor Devices*, (Wiley: New York), 1981.
32 Fleischer M, Ostrick B, Pohle R, Simon E, Meixner H, Bilger C & Daeche F, *Sens Actuators B*, 80 (2001) 169.
33 Revathy D, Govardhan K, Chella S, Tamilselvi G, Divyalakshmi S A, Ajita N, Ravi N, Natarajan P, Uma V, Amit B, Soon K J N & Andrews N G, *Microchimica Acta*, 12 (2017) 4765.
34 Imad H K, Abu H & Abdullah Q N, *Nano-Micro Lett*, 8 (2016) 20.
35 Liu Y, Tang W M & Lai P T, *Sens Actuators B*, 259 (2018) 725.
36 Je A W, Duy T P, Yong W J & Ki J J, *Int J Hydrogen Energy*, 29 (2017) 18754.
37 Zou Y, Wang Q, Jiang D, Cuili X, Chu H, Qiu S, Zhang H, Xu F, Sun L & Liu S, *Ceram Int*, 42 (2016) 8257.
38 Bharat S & Jung S K, *Int J Hydrogen Energy*, 42 (2017) 25446.
39 Bharat S & Jung S K, *Int J Hydrogen Energy*, 43 (2018) 11397.
40 Dae H B & Jongbaeg K, *Sens Actuators B*, 250 (2017) 686.
41 Tao W, Xiongbang W, Xiaohui Y, Yong Q, Guodong L, Yan S, Shuanghong W, Shibin L & Zhi Chen, *J Mater Sci: Mater Electron*, 28 (2017) 1428.